

A 3-D Microscale Model for CO₂ Gas Transport in Tomato Leaves during Photosynthesis

Q.T. Ho, P. Verboven, E. Herremans,
M.A. Retta, T. Defraeye and B.M. Nicolai
Flanders Center of Postharvest Technology
BIOSYST-MeBioS
Katholieke Universiteit Leuven
Willem de Croylaan 42, B-3001 Leuven
Belgium

Xinyou Yin, R.K. Thapa and P.C. Struik
Centre for Crop Systems Analysis
Wageningen University
P.O. Box 430, 6700 AK Wageningen
The Netherlands

Keywords: biophysical model, biochemical model, gas diffusion, mesophyll conductance

Abstract

Exchange of CO₂ in tomato (*Solanum lycopersicum* L.) leaves was modelled using combined gas diffusion and photosynthesis kinetics in a real 3-D geometric representation of the cellular microstructure, obtained by synchrotron radiation X-ray microtomography. The microscale model for gas exchange accounted for diffusive mass transport of CO₂ in the intercellular space (pores), the cell wall network and the intracellular liquid of cells. The photosynthesis kinetics described by the extended Farquhar, von Caemmerer & Berry model were coupled to the gas exchange inside the mesophyll cells. The coupled model was validated by means of gas exchange and chlorophyll fluorescence measurements. The model provides detailed insight into the mechanisms of gas exchange and insight into the effects of changes in ambient CO₂ concentration or photon flux density on stomatal and mesophyll conductance. The resistance to diffusion of CO₂ from the intercellular air spaces within the leaf through the mesophyll to the sites of carboxylation during photosynthesis depended on the 3-D microstructure of leaf tissue. The model represents an important step forward to study CO₂ diffusion coupled to photosynthesis at the leaf tissue level, taking into account its actual 3-D microstructure.

INTRODUCTION

Photosynthesis is amongst the most important metabolic processes in plants. During photosynthesis, CO₂ diffuses from the atmosphere into the leaf and finally to the site of carboxylation in the chloroplast stroma (Flexas et al., 2007). The diffusion of CO₂ through the leaves has been shown to be impeded by several conductances such as the regulation of the opening of the stomata and conductive properties of the mesophyll (Evans et al., 2009). The stomatal conductance (g_s) determines the gas exchange from the phyllosphere into the intercellular air space (von Caemmerer and Farquhar, 1981). The mesophyll conductance (g_m) is defined as the conductance for the transfer of CO₂ from the intercellular air space (C_i) to the site of carboxylation in the mesophyll cells (C_c). Correlations of the conductances with leaf structural properties have not always been clear (Flexas et al., 2007). Both g_s as well as g_m are apparent variables rather than physical constants as they implicitly incorporate microstructural and biochemical features of the tissue, cells and organelles that are involved in the gas transport mechanism.

Here, we describe a microscale model for CO₂ exchange through the leaf by coupling a biophysical model of gas diffusion to the biochemical model of photosynthesis. The diffusion model accounted for mass transport of CO₂ in the intercellular space (pores), the cell wall network and the intracellular liquid of cells. The photosynthetic kinetics described by the extended Farquhar, von Caemmerer & Berry (FvCB, Farquhar et al., 1980) model was incorporated into the gas transport equations. The model can be used to quantify the importance of the different pathways of gas exchange, and to analyze the response of the net photosynthesis A and conductance g_m to environmental factors such as CO₂ and irradiance. Tomato (*Solanum lycopersicum* L.)

leaf was chosen as the model system.

MATERIALS AND METHODS

Photosynthetic Kinetics Model

The FvCB model was used in this study to describe the gross CO₂ fixation rate A_G in the chloroplasts of tomato plants (Farquhar et al., 1980; von Caemmerer, 2000). Briefly,

$$A_G = \min(A_{G,c}, A_{G,j}, A_{G,p}) \quad (1)$$

where $A_{G,c}$ = the Rubisco-limited rate, $A_{G,j}$ = the RuBP(Ribulose-1,5-bisphosphate) regeneration or electron transport limited rate, and $A_{G,p}$ = the triose phosphate utilization (TPU) limited rate of CO₂ assimilation. $A_{G,c}$, $A_{G,j}$ and $A_{G,p}$ were calculated from

$$A_{G,c} = \frac{(C_c - \Gamma^*)V_{c,max}}{C_c + K_{m,C}(1 + O_2 / K_{m,O_2})} \quad (2)$$

$$A_{G,j} = \frac{(C_c - \Gamma^*)J}{4C_c + 8\Gamma^*} \quad (3)$$

$$A_{G,p} = 3T_p \quad (4)$$

where C_c and O_2 are the CO₂ and O₂ concentration in the chloroplast, respectively; J is the rate of electron transport; T_p is the rate of triose phosphate export from the chloroplast; and Γ^* is the CO₂ compensation point in the absence of respiration. $K_{m,C}$, K_{m,O_2} and $V_{c,max}$ are constants of Rubisco activity-limited carboxylation. The net photosynthesis rate A was defined as $A = A_G - R_d$, where R_d is the respiratory CO₂ release other than by photorespiration. For further details, refer to Yin et al. (2009).

Gas Exchange and Chlorophyll Fluorescence Measurements

'Admiro' cultivar was used for photosynthesis measurements. Plants were grown under natural plus supplemental light and the photoperiod was 16 hours per day. Simultaneous gas exchange and chlorophyll fluorescence measurements at both 21% and 2% O₂ were performed at the beginning of the flowering stage, using an open gas exchange system (Li-Cor 6400; Li-Cor Inc, Lincoln, NE, USA) and an integrated fluorescence chamber head (LI-6400-40; Li-Cor Inc, Lincoln, NE, USA). Measurements were carried out on four plants; we selected the distal-side leaflets from the top-most fully expanded leaf and from the fourth leaf below the top-most fully grown leaf for measurements. All measurements were made at a leaf temperature of 25°C and a leaf-to-air vapour pressure difference of 1.0-1.6 kPa. For the C_i (intercellular CO₂ partial pressure) response curves, the ambient air CO₂ concentration (C_a) was increased step-wise: 50, 100, 150, 200, 250, 350, 500, 650, 1000, and 1500 $\mu\text{mol mol}^{-1}$, while keeping incident irradiance I_{inc} at 1000 $\mu\text{mol m}^{-2} \text{s}^{-1}$. For the I_{inc} response curves, the photon flux densities were in a series: 0, 20, 65, 100, 150, 200, 500, 1000, 1500, 2000 $\mu\text{mol m}^{-2} \text{s}^{-1}$, while keeping C_a at 380 $\mu\text{mol mol}^{-1}$ for measurements at 21% O₂, and keeping C_a at 1000 $\mu\text{mol mol}^{-1}$ for measurements at 2% O₂ to ensure a non-photorespiration condition. The photosynthetic parameters of the FvCB model were estimated using method described by Yin et al. (2009) and are given in Table 1.

Microscale Gas Exchange Model

Microscale diffusion was assumed to dominate transport in each of the pores and cells, while in the chloroplasts, photosynthesis was assumed to take place. Microscale diffusion in air pores and cells can be described by:

$$\frac{\partial C_{CO_2,i}}{\partial t} = \nabla \cdot D_{CO_2,i} \nabla C_{CO_2,i} - \frac{A}{d \cdot f_c} + \frac{R_d}{d \cdot f_m} + B \quad (5)$$

$$\frac{\partial C_{HCO_3^-,c}}{\partial t} = \nabla \cdot D_{HCO_3^-,c} \nabla C_{HCO_3^-,c} - B \quad (6)$$

where the index i indicates the gas phase of the pores (g) or the liquid phase of the cells (l). $C_{CO_2,i}$ (mol m⁻³) is the O₂ concentration in phase i , ∇ is the gradient operator (m⁻¹) and $D_{CO_2,i}$ (m² s⁻¹) is the CO₂ diffusivity in phase i , d (m) is the leaf thickness while f_c and f_m are the fractions of chloroplasts and cytosols of the leaf, respectively. The second term in Equation (5) is the volumetric CO₂ consumption by photosynthesis (described by the FvCB model) in the chloroplasts while the third term is the volumetric CO₂ production by respiration of mitochondria in the cytoplasm. The last term of Equations (5) and (6) is the net hydration rate of CO₂ to HCO₃⁻:

$$B = k_2 \frac{[H]^+ C_{HCO_3^-,c}}{K} - k_1 C_c \quad (7)$$

where k_1 , k_2 and K are the rate constants of the CO₂ to HCO₃⁻ conversion (for further details see Ho et al., 2011). The relationship between the equilibrium CO₂ concentration in the gas and liquid phase was assumed to be described by Henry's law. The resistance to the gas transport of the cell wall and cell membrane was taken into account at the interface between gas and liquid phase. Values of the physical properties that appear in the microscale model are given in Table 2.

Leaf Microstructure

The synchrotron X-ray computed tomography experiment of tomato (*Solanum lycopersicum*) leaves was performed at the European Synchrotron Radiation Facility in Grenoble, France. The 3-D microstructure of tomato leaf tissues were reconstructed from a series of slices of tomography images using Avizo image-processing software (Visualization Group Sciences). Further organelles inside the mesophyll cells were explicitly reconstructed. For simplicity, chloroplasts were modelled as a layer of 2.6 μm located beneath the boundary of the mesophyll cell. The vacuoles were modelled explicitly in the mesophyll cells by shrinking the cell volume by 70% and considering the shrunk volume to be vacuole. The layer between the chlorophyll layer and the tonoplast was considered to be cytoplasm.

Numerical Solution

The model for CO₂ diffusion was solved on the 3-D geometry using the finite volume method (Versteeg and Malalasekera, 1995). 3-D tomographic images of leaf tissue samples (127.5×127.5×195 μm) were discretized into 7.514×10⁶ cube elements with axes of 0.75 μm. The model equations were discretized over the finite volume grid to yield a linear system of algebraic equations on the unknown concentrations at the nodes. The linear equation system was solved by the preconditioned conjugate gradient procedure available in Matlab (The Mathworks) on a 16-GB RAM node of the High-Performance Computer in the VSC – Flemish Supercomputer Center.

RESULTS

Microscopic Gas Concentration Distribution

The microscale model confirmed that there are indeed CO₂ gradients inside the leaf tissue. Figure 1 shows the simulation results of 3-D microscale CO₂ gas transport performed on tissue samples that were 164 μm thick (lower leaf) and 131 μm thick (upper leaf). Since the epidermis has a low permeability, transport of CO₂ occurred mostly through stomata. Tomato leaves have a large intercellular space (30-44%) and high connectivity resulted in a uniform CO₂ concentration of intercellular space. Clearly, the CO₂ concentration is low inside the cells. The chloroplasts were modelled as layers adhering to the mesophyll wall. CO₂ concentration gradient was found especially at the

sites where cells touch each other.

Photosynthesis in Response to CO₂ Concentration

In a next step, we investigated whether the microscale model was able to predict the measured response of leaf photosynthesis to the ambient CO₂ concentration in photorespiration conditions. Figures 2a and b show the results of the measured and simulated net photosynthesis rate at different intercellular CO₂ concentrations (C_i), photon flux density incident on leaves of 1000 $\mu\text{mol m}^{-2} \text{s}^{-1}$ and 21% O₂. A good agreement was found between measured and simulated data. Both model and measured results predicted that the net photosynthesis of leaves rapidly increased at low C_i concentrations but saturated at high CO₂ concentrations. In Figures 2c and d, the mesophyll conductance g_m is plotted as a function of C_i . Excluding the low-CO₂ region where any assessment of g_m is uncertain, clearly the measured mesophyll conductance decreased with increasing CO₂ levels. The modelled results indicated that mesophyll conductance also decreased with increasing CO₂ levels but then stabilized at high CO₂ concentrations.

Photosynthesis of Upper and Lower Leaves

Upper leaves and lower leaves are different in photosynthesis capacity and morphology characteristics. Synchrotron X-ray computed tomography experiments indicated that upper leaves were thinner than lower leaves. Mesophyll cells of upper leaves were smaller than those of lower leaves. Gas exchange and chlorophyll fluorescence measurements showed that the photosynthesis capacity of upper leaves was higher than that of lower leaves (Figs. 2a and b). Both simulations and measurements indicated that the mesophyll conductance of upper leaves was higher than that of the lower leaves (Table 3). A good agreement between the modelled and measured results was observed.

DISCUSSION

Several authors have used the reaction diffusion model to describe CO₂ uptake by leaves (Vesala et al., 1996; Aalto and Juurola, 2002). Such models were solved with geometrical simplifications, for example by assuming CO₂ diffusion through a single stomaton and the surrounding mesophyll using an axial symmetry model (Vesala et al., 1996), or by implementing a 3-D model for CO₂ gas exchange through the leaf but using basic geometrical elements such as spheres and cylinders representing mesophyll cells (Aalto and Juurola, 2002). While in the latter model the cells were separated by air gaps (Aalto and Juurola, 2002), in reality cells touch each other and this contact may reduce both the surface available for CO₂ exchange and the diffusion among the cells as we have clearly shown. The most realistic photosynthesis model to date was recently described by Tholen and Zhu (2011). Their model, while addressing 3-D CO₂ transport in a single mesophyll cell and incorporating subcellular features such as chloroplasts and mitochondria, does not account for any resistances due to the leaf microstructure and in particular the mesophyll. In this current model, we incorporated for the first time the actual microstructure as observed from synchrotron X-ray computed tomography experiments in the CO₂ transport model. This model confirmed the effect of mesophyll cells touching each other and thereby reducing the exchange surface between mesophyll and intercellular space. A large CO₂ gradient was found in the palisade mesophyll cells beneath the adaxial epidermis layer and contact surface between the mesophyll cells. Simulations with our model suggest that in tomato leaves, the actual microstructure indeed affects gas transport and mesophyll conductance in particular. Note that Tholen and Zhu (2011) did not address an important part of the gas exchange pathway – that from the ambient atmosphere through the stomata and the intercellular space towards the mesophyll cell.

The model predicted net photosynthesis similar to the measured values. The measured mesophyll conductance decreased with increasing CO₂ levels. The modelled

mesophyll conductance also decreased with increasing CO₂ levels but then stabilized at high CO₂ concentration. Note that the measured mesophyll conductance was estimated by assuming that the CO₂ assimilation was limited by the electron transport rate. However, the method using combined gas exchange and chlorophyll fluorescence data to estimate CO₂ concentration of chloroplast (C_c) and mesophyll conductance (g_m) may not be reliable at high ambient CO₂ concentration where most likely triosephosphate utilisation limits photosynthesis. On the other hand, a discrepancy of the mesophyll conductance at high CO₂ levels may indicate that some physiological processes related to photosynthesis are not incorporated in the model.

CONCLUSIONS

Gas exchange in tomato leaves during photosynthesis was investigated by combining a microscale gas diffusion model with a model of photosynthetic kinetics. The combined model incorporated the actual 3-D tissue microstructure of the tomato leaf, which was derived from synchrotron X-ray computed images. The conductance of CO₂ from the intercellular airspaces within the leaf through the mesophyll to the sites of carboxylation during photosynthesis was dependent on the 3-D microstructure of leaf tissue. The upper leaves showed higher photosynthesis capacity and mesophyll conductance compared to the lower leaves. The model represents an important step forward to studying CO₂ diffusion coupled to photosynthesis at the leaf tissue level, taking into account its actual 3-D microstructure.

ACKNOWLEDGEMENTS

The authors wish to thank the Research Council of the K.U. Leuven (OT 08/023), the Research Fund Flanders (project G.0603.08), and the Institute for the Promotion of Innovation by Science and Technology in Flanders (project IWT-050633) for financial support. Wageningen based authors have contributed to this work within the programme BioSolar Cells. Quang Tri Ho is a postdoctoral fellow of the Research Fund Flanders (FWO Vlaanderen).

Literature Cited

- Aalto, T. and Juurola, E. 2002. A three-dimensional model of CO₂ transport in airspaces and mesophyll cells of a silver birch leaf. *Plant, Cell Environ.* 25:1399-1409.
- Bernacchi, C.J., Portis, A.R., Nakano, H., von Caemmerer, S. and Long, S.P. 2002. Temperature response of mesophyll conductance. Implications for the determination of Rubisco enzyme kinetics and for limitations to photosynthesis in vivo. *Plant Physiol.* 130:1992-1998.
- Einstein, A. 1905. On the movement of small particles suspended in stationary liquids required by the molecular-kinetic theory of heat. *Ann. Phys.* 17:549-560.
- Evans, J.R., Kaldenhoff, R., Genty, B. and Terashima, I. 2009. Resistances along the CO₂ diffusion pathway inside leaves. *J. Exp. Bot.* 60:2235-2248.
- Farquhar, G.D., von Caemmerer, S. and Berry, J.A. 1980. A biochemical model of photosynthetic CO₂ assimilation in leaves of C₃ species. *Planta* 149:78-90.
- Flexas, J., Diaz-Espejo, A., Galmes, J., Kaldenhoff, R., Medrano, H. and Ribas-Carbó, M. 2007. Rapid variation of mesophyll conductance in response to changes in CO₂ concentration around leaves. *Plant, Cell Environ.* 30:1284-1298.
- Frost-Christensen, H. and Floto, F. 2007. Resistance to CO₂ diffusion in cuticular membranes of amphibious plants and the implication for CO₂ acquisition. *Plant, Cell Environ.* 30:12-18.
- Geers, C. and Gros, G. 2000. Carbon dioxide transport and carbonic anhydrase in blood and muscle. *Physiol. Rev.* 80:681-715.
- Gutknecht, J., Bisson, M.A. and Tosteson, F.C. 1977. Diffusion of carbon dioxide through lipid bilayer membranes: effect of carbonic anhydrase, bicarbonate, and unstirred layers. *J. Gen. Physiol.* 69:779-794.
- Ho, Q.T., Verboven, P., Verlinden, B.E., Herremans, E., Wevers, M., Carmeliet, J. and

- Nicolai, B.M. 2011. A 3-D multiscale model for gas exchange in fruit. *Plant Physiol.* 155:1158-1168.
- Jolly, W.L. 1985. *Modern Inorganic Chemistry*. McGraw-Hill, New York.
- Lide, D.R. 1999. *Handbook of Chemistry and Physics*. CRC Press, New York.
- Tholen, D. and Zhu, X.G. 2011. The mechanistic basis of internal conductance: a theoretical analysis of mesophyll cell photosynthesis and CO₂ diffusion. *Plant Physiol.* 156:90-105.
- Versteeg, J.K. and Malalasekera, W. 1995. *An Introduction to Computational Fluid Dynamics*. Longman Scientific & Technical, Harlow, UK.
- Vesala, T., Ahonen, T., Hari, P., Krissinel, E. and Shokhirev, N. 1996. Analysis of stomatal CO₂ uptake by a three-dimensional cylindrically symmetric model. *New Phytol.* 132:235-245.
- von Caemmerer, S. 2000. *Biochemical Models of Leaf Photosynthesis*. Techniques in Plant Sciences No. 2. CSIRO Publishing, Collingwood, Victoria, Australia.
- von Caemmerer, S. and Farquhar, G.D. 1981. Some relationships between the biochemistry of photosynthesis and the gas-exchange of leaves. *Planta* 153:376-387.
- Yin, X., Struik, P.C., Romero, P., Harbinson, J., Evers, J.B., Van Der Putten, P.E.L. and Vos, J. 2009. Using combined measurements of gas exchange and chlorophyll fluorescence to estimate parameters of a biochemical C₃ photosynthesis model: A critical appraisal and a new integrated approach applied to leaves in a wheat (*Triticum aestivum*) canopy. *Plant, Cell Environ.* 32:448-464.

Tables

Table 1. Values (\pm standard error of estimate if applicable) of photosynthetic parameters estimated for ‘Admiro’ tomato leaves.

Parameters	Upper leaves	Lower leaves
$V_{c,max}$ ($\mu\text{mol m}^{-2} \text{s}^{-1}$)	133.6 \pm 13.68	57.94 \pm 3.08
$K_{m,C}$ (μbar) *	267	267
$K_{m,O}$ (mbar) *	164	164
S	0.473	0.429
Γ^* (μbar)	33.52	33.52
R_d -common ($\mu\text{mol m}^{-2} \text{s}^{-1}$)	1.784	0.933
R_{dk} ($\mu\text{mol m}^{-2} \text{s}^{-1}$)	2.611	2.431
T_p ($\mu\text{mol m}^{-2} \text{s}^{-1}$)	9.04 \pm 0.30	8.1

*Value is given by Bernacchi et al. (2002).

Table 2. Physical parameters of the microscale gas exchange model. Diffusion in the liquid phase was assumed to follow the Stokes-Einstein law (inversely related to the kinematic viscosity of the solvent, Einstein, 1905), $D_{CO_2,l} = D_{CO_2,water}/\eta$.

Model parameters	Symbol	Values
Diffusivity		
- Pore	$D_{CO_2,g}$	$1.60 \times 10^{-5} \text{ m}^2 \text{ s}^{-1}$ at 20°C ^a
- Cell	$D_{CO_2,water}$	$1.67 \times 10^{-9} \text{ m}^2 \text{ s}^{-1}$ at 20°C ^a
	$D_{HCO_3^-,c}$	$1.17 \times 10^{-9} \text{ m}^2 \text{ s}^{-1}$ ^b
Cuticular membrane permeability	P_{cuti}	$7 \times 10^{-6} \text{ m s}^{-1}$ ^c
Cellular membrane permeability	P_{mem}	$3.5 \times 10^{-3} \text{ ms}^{-1}$ ^d
Henry's constant	H	$0.83 \text{ (mol m}^{-3} \text{ liquid)(mol m}^{-3} \text{ gas)}^{-1}$ at 25°C ^a
CO ₂ reaction rate constants	k_1	0.039 s^{-1} ^e
	k_2	23 s^{-1} ^e
	K	$2.5 \times 10^{-4} \text{ mol L}^{-1}$ ^e
Cytosol viscosity	η	2 (relative to water) ^f
Stroma viscosity	η	2 (relative to water)

^aLide (1999), ^bFrost-Christensen and Floto (2007), ^cGeers and Gros (2000), ^dGutknecht et al. (1977), ^eJolly (1985), and ^fTholen and Zhu (2011).

Table 3. Mesophyll conductance (g_m) calculated from measurement and simulation. R_d and R_{dk} are day respiration and dark respiration (further details are described by Yin et al., 2009). From combined gas exchange and chlorophyll measurements, mesophyll conductance was calculated with different R_d -common and R_{dk} .

	R_d	C_a ($\mu\text{mol mol}^{-1}$)	g_m ($\text{mol m}^{-2} \text{ s}^{-1}$)	
			Lower leaves	Upper leaves
Measurement	R_d -common	350	0.120	0.183
	R_{dk}	350	0.158	0.204
Simulation	R_d -common	350	0.161	0.214
	R_{dk}	350	0.161	0.213

Figures

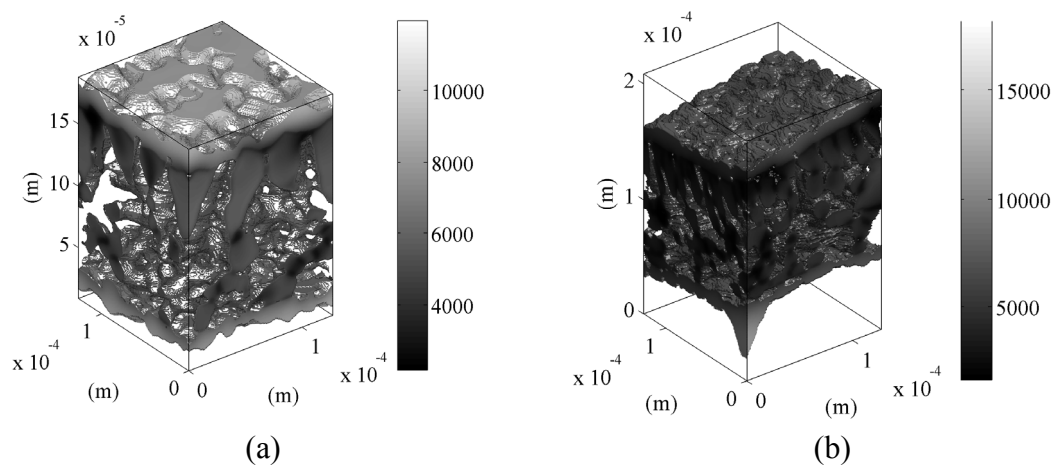


Fig. 1. Computed intra cellular CO_2 distribution in a tomato leaf ('Admiro'). The ambient conditions were $350 \mu\text{mol mol}^{-1}$ CO_2 , 21% O_2 , photon flux density incident irradiance (I_{inc}) of $1000 \mu\text{mol m}^{-2} \text{s}^{-1}$ and 25°C . Concentrations are expressed in $\mu\text{mol m}^{-3}$. (a) and (b) are upper and lower leaves, respectively.

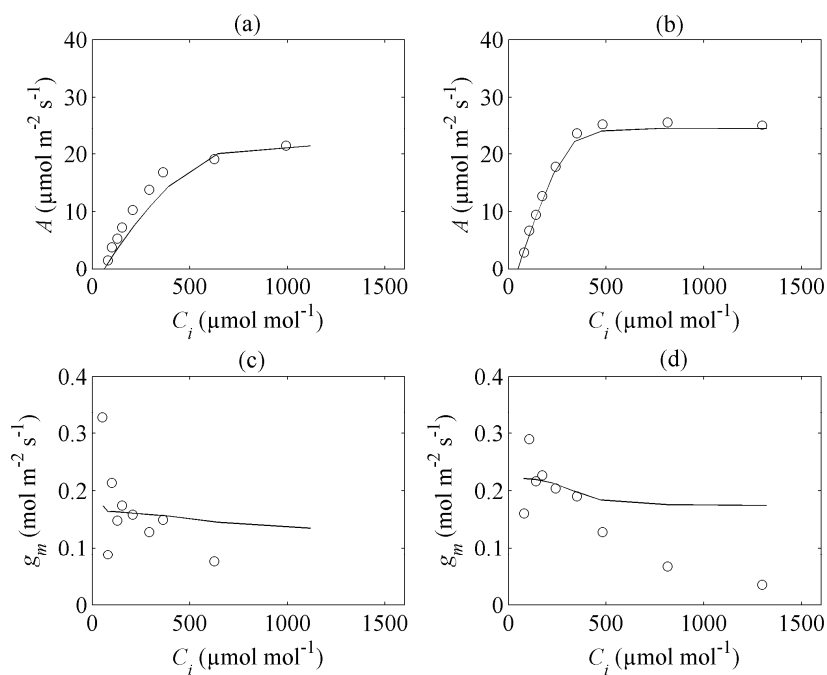


Fig. 2. Simulations and measurements of photosynthesis of tomato 'Admiro' leaves at different conditions of intercellular CO_2 concentration C_i at 21% O_2 , photon flux density incident to leaves I_{inc} of $1000 \mu\text{mol m}^{-2} \text{s}^{-1}$ and 25°C . Panels (a) and (b) show net photosynthesis A as function of C_i of upper and lower leaves, respectively. Panels (c) and (d) show mesophyll conductance g_m as function of C_i for upper and lower leaves. The symbols represent measurements while the lines indicate model predictions.